Effect of Blending Sequence on the Morphologies of Poly(butylene terephthalate)/Epoxy/Clay Nanocomposites by a Rheological Approach

Defeng Wu, Chixing Zhou, Wei Yu, Fan Xie

School of Chemistry and Chemical Technology, Shanghai Jiaotong University, Shanghai 200240, China

Received 21 March 2005; accepted 9 May 2005
DOI 10.1002/app.22215
Published online in Wiley InterScience (www.interscience.wiley.com).

ABSTRACT: Epoxy resin was used as a compatilizer to prepare poly(butylene terephthalate)/clay nanocomposites via melt intercalation. Three different mixing sequences were attempted in the present work: (1) to mix poly(butylene terephthalate) (PBT), epoxy, and organoclay in one step; (2) first to mix epoxy and organoclay, and then mix it with PBT; (3) to prepare PBT/organoclay hybrid first, and then mix it with epoxy to get the final nanocomposites. The results from X-ray diffraction (XRD) reveal that all these hybrids present an intercalated structure. However, it can be observed that there are distinct differences in the amount and average size of clay tactoids dispersed in those hybrids from the transmission electron microscope (TEM) photographs, which are further confirmed successfully by the rheological measurements. On the basis of the strain overshoot intensity and the low-frequency solid-like response level in the small amplitude oscillatory shear (SAOS) measurements, it can be concluded that the blending sequence (2) is the best way to obtain a nice dispersion of clay in the matrix, forming a percolated tactoids network with highest density and intensity. © 2005 Wiley Periodicals, Inc. J Appl Polym Sci 99: 340–346, 2006

Key words: poly(butylene terephthalate); nanocomposites; blending sequence; rheology; morphologies

INTRODUCTION

Poly(butylene terephthalate) (PBT) is a typical semicrystalline polymer and an engineering plastic, with excellent mechanical properties, which has found wide application in fibers and moldings. Many research studies have concentrated on blending PBT with another polymer or with one of a variety of fillers to obtain new polymeric materials with desirable properties.[1–3]

The use of layered-aluminosilicates as fillers in polymers has received considerable attention in recent years. Studies have repeatedly shown that dispersing individual high-aspect-ratio silicate platelets leads to marked property enhancements. A large number of polymers with varying degrees of polarity and chain rigidity have been used as matrices for polymer/clay nanocomposites, including polyamide,[4–6] polystyrene,[7,8] polypropylene,[9–13] polyimides,[14] epoxy resin,[15] polyurethane,[16] poly(ethylene terephthalate),[17] and so on.

The layered silicate was also used as a modifying agent to obtain a PBT nanocomposite with property enhancements.[18–23] Li et al.[18] first prepared an intercalated PBT/montmorillonite nanocomposite via melt intercalation. An exfoliated sulfonated PBT/clay hybrid was obtained by Chisholm et al.,[19] and they attributed the influence of ionic groups on exfoliation to an ionic interaction between the negatively charged ionomer and the positively charged edge surfaces of the montmorillonite (MMT) platelets. A further study on the effect of blending sequence on the properties and morphologies of PBT/EVA-g-MAH/clay ternary nanocomposites was conducted by Li,[20] mainly using conventional methods of X-ray diffraction (XRD) and transmission electron microscope (TEM). They found that the mixing sequence significantly influenced the microstructure of the hybrids and the dispersion states of the organoclay in the polymer matrix.

Recently, rheometry has been proved to be a powerful tool for investigating the internal microstructures of nanocomposites[7,11–13] such as the state of dispersion of clay and, the confinement effect of silicate layers on the motion of polymer chains. In our previous work, we studied the rheological behavior of the intercalated PBT/clay nanocomposites and found that the formation of the liquid–crystalline-like phase structure in the nanocomposites might be the major drive force for the reorganization of the internal network.[21] Then, to improve the dispersion of clay in the PBT matrix, we

Correspondence to: C. Zhou (cxzhou@sjtu.edu.cn).
Contract grant sponsor: National Natural Science Foundation of China; contract grant numbers: 20174024 and 50290090.

TABLE I
Blending Sequence and Abbreviation of the Prepared Hybrids

Blending sequence	Abbreviation
PBT + E51 + DK2[a]	BEM
PBT + (E51 + DK2)[a]	B-EM
(PBT + DK2) + E51	BM-E
PBT + DK2[a]	BM

[a] To keep the same thermal history with BM-E, these samples were mixed twice in a Rheomix-600 mixer.

used the epoxy resin as a compatilizer preparing the PBT/clay nanocomposites by direct melt compounding. The results from the rheology and properties characterization indicated that the epoxy content influenced the phase morphologies and properties of the nanocomposites remarkably.[22] In the present work, at first, we prepared the PBT/clay nanocomposites, using the epoxy resin as a compatilizer by different mixing sequence, and then conducted a rheological study on these nanocomposites. This investigation aims at relating the linear rheological behaviors to the effect of blending sequence on the morphologies of the nanocomposites.

EXPERIMENTAL

Materials

The PBT (1097A, M_n = 23,200) used in this study is a commercial product of Nantong XinChen Synthetic Material, P. R. China. The organoclay (trade name is DK2) with particle size of <50 μm was supplied by Zhejiang FengHong Clay, China, modified with methyl tallow bis(2-hydroxyethyl) ammonium. The epoxy resin used was E51, a bisphenol A diglycidyl ether-based resin made by Shanghai Synthetic Resin, P. R. China. Its average molecular weight is about 390 g/mol and the epoxide equivalent weight is about 0.51 g/equiv.

Sample preparation

Three different mixing sequences were attempted in the present work: to mix PBT, E51, and DK2 in one step; first to mix E51 and DK2 at 80°C for 30 min, then to mix it with PBT; and to prepare PBT/DK2 hybrid first, then mix it with E51 to get the final nanocomposites. All the samples were composed of DK2 in 4 wt % and E51 in 8 wt % and prepared by melt intercalation in a Rheomix-600 mixer (Haake Rheocord 900, Germany) at 230°C and 50 rpm for 8 min. Moreover, a blank sample without addition of E51 was prepared under the same experimental condition for a comparison. The abbreviation of these hybrids was listed in Table I. All the materials were dried at 80°C under vacuum for 24 h before using.

X-ray diffractometry characterization

The degree of swelling and the interlayer distance of the clay in the PCN hybrids were determined by X-ray diffractometer (XRD). The experiments were performed using a Rigaku Dmax-rC diffractometer with Cu target and a rotating anode generator operated at 40 kV and 100 mA. The scanning rate was 2°/min from 1° to 10°. The film sample for XRD measurement was prepared by compression molding at 230°C and 10 MPa.

Figure 1 shows the XRD patterns of DK2 and the PBT/clay nanocomposites prepared by different blending sequence. Compared with that of the BM sample, the d_{001} peaks of BM-E, BEM, and B-EM hybrids shift to lower angles in some extent, and the interlayer spacing of clay increases to 3.86, 4.00, and 4.80 nm, respectively. In the melt process, epoxy molecule acts as a compatilizer due to the strong polarity of its epoxide groups. Those epoxy molecules adhering to the clay surface further reduce the surface energy of clay particles and improve the compatibility between the matrix and clay. Accordingly, PBT chains are easier to intercalate into the gallery of the clay, in comparison with that of BM hybrid, which results in increase in the interlayer spacing of clay. It is notable that B-EM sample presents highest swollen level of clay, while the interlayer spacing of clay in BEM and BM-E samples are slightly lower. Compared with that of B-EM, the diffusion of epoxy molecules into matrix and clay in the mixing progress of BEM and BM-E hybrids is influenced by the blending sequence. As for B-EM hybrid, however, the first step of premixing epoxy and clay can make the most of primary clay particles soaked or swollen richly because of the strong interactions between polar epoxide group and

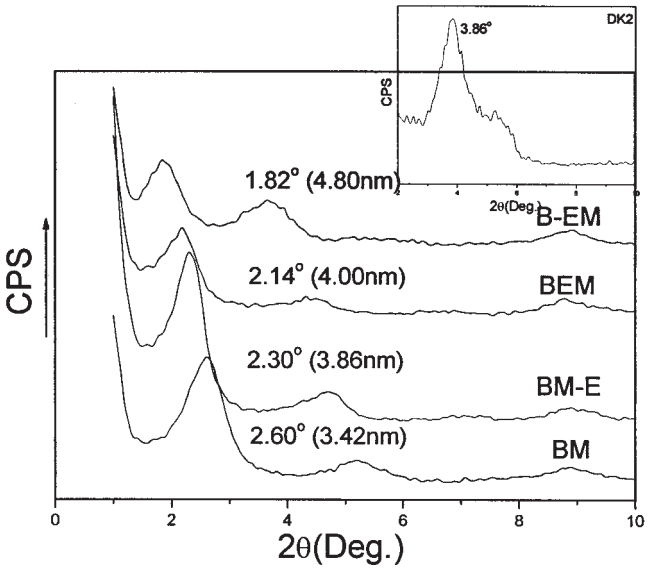

Figure 1 XRD patterns for the clay and hybrids.

hydroxyl group on the surfactant or basal surface of clay. As a result, in the later melt process, more PBT chains can intercalate into the clay galleries. Moreover, the increased environmental enthalpy around tactoids, due to the chain extension reaction between PBT matrix and epoxy molecules,[24] is a reasonable factor resulting in increasing in interlayer distance of tactoids in B-EM sample. Although the differences in interlayer spacing among BEM, BM-E, and B-EM hybrids suggest that the blending sequence may influence the dispersion of clay in the PBT matrix, all the hybrids present a distinct intercalated structure, however.

Transmission electron microscope characterization

The transmission electron micrographs were taken from 80 to 100 nm thick, microtomed sections, using a transmission electron microscope (TEM) (HITACHI H-860, Japan) with 100 kV accelerating voltage.

Rheological measurements

Rheological measurements were carried out in an oscillatory mode on a rheometer (Gemini 200 rheometer, Bohlin, UK) equipped with a parallel plate geometry using 25 mm diameter plates at 230°C. All measurements were performed with a 200 FRTN1 transducer with a lower resolution limit of 0.02 g cm. The samples about 1.0 mm in thickness were prepared by compression molding. Before testing, all samples suffered a quiescent annealing process for 30 min at 230°C under a nitrogen atmosphere in the parallel plate fixture. In the linear viscoelastic measurements, the small amplitude oscillatory shear (SAOS) was applied, and the dynamic strain scan measurements and the dynamic frequency scan measurements were carried out.

RESULTS AND DISCUSSION

The dynamic strain sweep was first conducted to determine the linear viscoelastic region of the samples. Figure 2 shows the dependence of normalized dynamic storage modulus of the PBT/clay nanocomposites on the strain (γ_0). Compared with that of BM hybrids, the linear viscoelastic region of BEM, BM-E, and B-EM hybrids lengthens. With the addition of epoxy as a compatilizer, the compatibility between PBT matrix and clay is enhanced. As a result, there are more PBT chains randomly tangled around the clay tactoids than that in BM hybrid, leading to the extension of the linear viscoelastic region. After critical strain values, the curves all drop down, showing shear thinning behavior, which is a typical feature of entangled polymeric materials.

Furthermore, the BEM, BM-E, and B-EM hybrids show a weak strain overshoot, as can be seen in the part covered by the ellipse in Figure 2. It suggests that some weak bonds exist between PBT chains and nanoclay. In our previous work,[25] the hydrogen bonding has been detected in melt state of BEM hybrid through in situ FTIR spectroscopy experiment. The carbonyl groups in PBT can form hydrogen bonds with (a) hydroxyl group in those epoxy adhering on the surface of tactoids, (b) those yielded hydroxyl groups in copolymer (yielded from the chain extension reaction between PBT and epoxy[24,25]) chains confined by tactoids or not, and (c) hydroxyl group of the clay layers. It is notable that the B-EM hybrid presents the strongest strain overshoot, as shown in the amplificatory image of Figure 2. As mentioned above, the first step of premixing epoxy and clay in B-EM hybrid preparation can make the most of primary clay particles soaked or swollen richly by the polar epoxy molecules and, as a result, in the later melt process, more PBT chains can intercalate into the clay galleries and many smaller tactoids may detach from the big one due to the nice compatibility between PBT and epoxy. Therefore, those epoxy molecules adhering on the surface of tactoids can form hydrogen bonds with PBT chains; on the other hand, the formation of more clay tactoids results in an increase in phase contact area, strengthening the hydrogen bonding between PBT chain and tactoids. According to the overshoot strength, it can be expected that the role of compatilizer played by epoxy in BEM is better than that in BM-E hybrid. The results mentioned above suggest that the differences in physical adsorption and hydrogen bonding between PBT chains and tactoids will influence the final morphologies of those hybrids prepared by different mixing sequence.

To further investigate the blending sequence on the morphologies of PBT/clay nanocomposites, the dynamic frequency scan measurements were carried out, and the curves of the storage modulus for these hy-

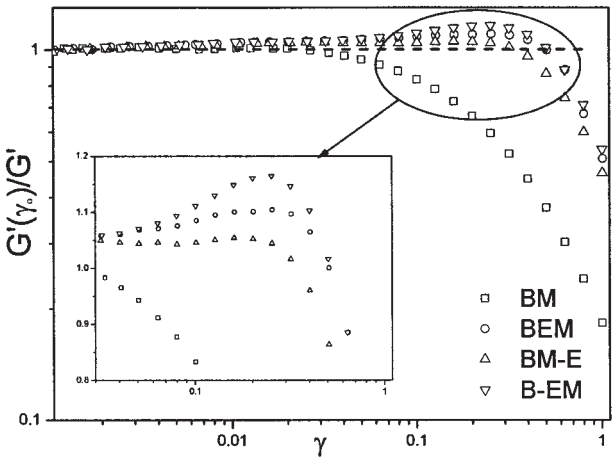

Figure 2 Strain dependence of the normalized storage modulus of the hybrids at $T = 230$°C and $\bar{\omega}$=1 Hz.

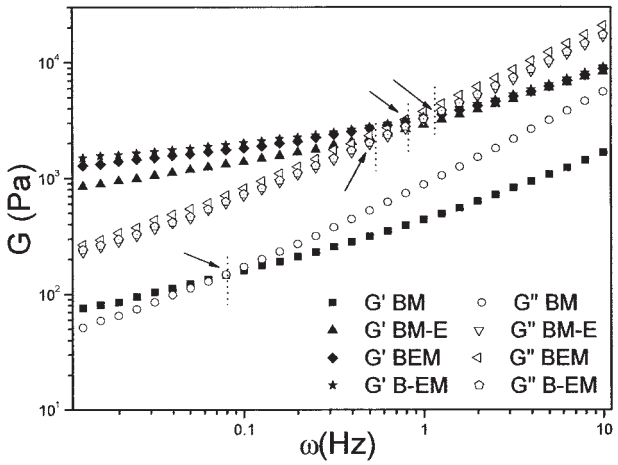

Figure 3 Comparison of dynamic storage modulus and loss modulus of the hybrids.

brids are compared in Figure 3. All the samples display an unterminal behavior at low frequencies, and it is obvious that with the addition of the epoxy, the dependencies of the storage modulus, G', for the BEM, BM-E, and B-EM hybrids on the frequency, ω, decrease sharply in the terminal zone, and the G' curves exhibit a plateau more distinctly at the low frequencies in contrast to that of BM hybrid. Additionally, it is noteworthy that the low-frequency storage moduli of the BEM, BM-E, and B-EM hybrids are not equal to one another, and can be ordered as $G'_{B-EM} > G'_{BEM} > G'_{BM-E}$. On XRD results, the interlayer spacing of BM-E, BEM, and B-EM hybrids is 3.86, 4.00, and 4.80 nm, respectively. Therefore, it can be thought that polymer chains intercalated into silicate interlayer must be confined between parallel walls separated by a distance smaller than or of the same order of the size of the chain coils. With increasing in the swollen degree of clay tactoids, more polymer chains will be confined leading to the change of the relaxation dynamics of polymer, which seems to be able to explain the increase in low-frequency modulus. However, it has been proven that the solid-like rheological response at low frequencies does not arise from confinement of chains, but from the formation of percolated clay networks resulting from the interactions between the clay tactoids themselves, and the dispersion states of the clay have great effects on the percolation strength.[11–13] Therefore, the results from Figure 3 suggest that different dispersion states of clay tactoids, such as the size and amount, might exist in these three hybrids.

To confirm the dispersion state of the clay in the matrix, Figures 4(a–d) gives the TEM image of all the hybrids at a magnification of 20,000×. Compared with BM hybrid, BM-E hybrid still presents an intercalated structure, while the average size of the tactoids in

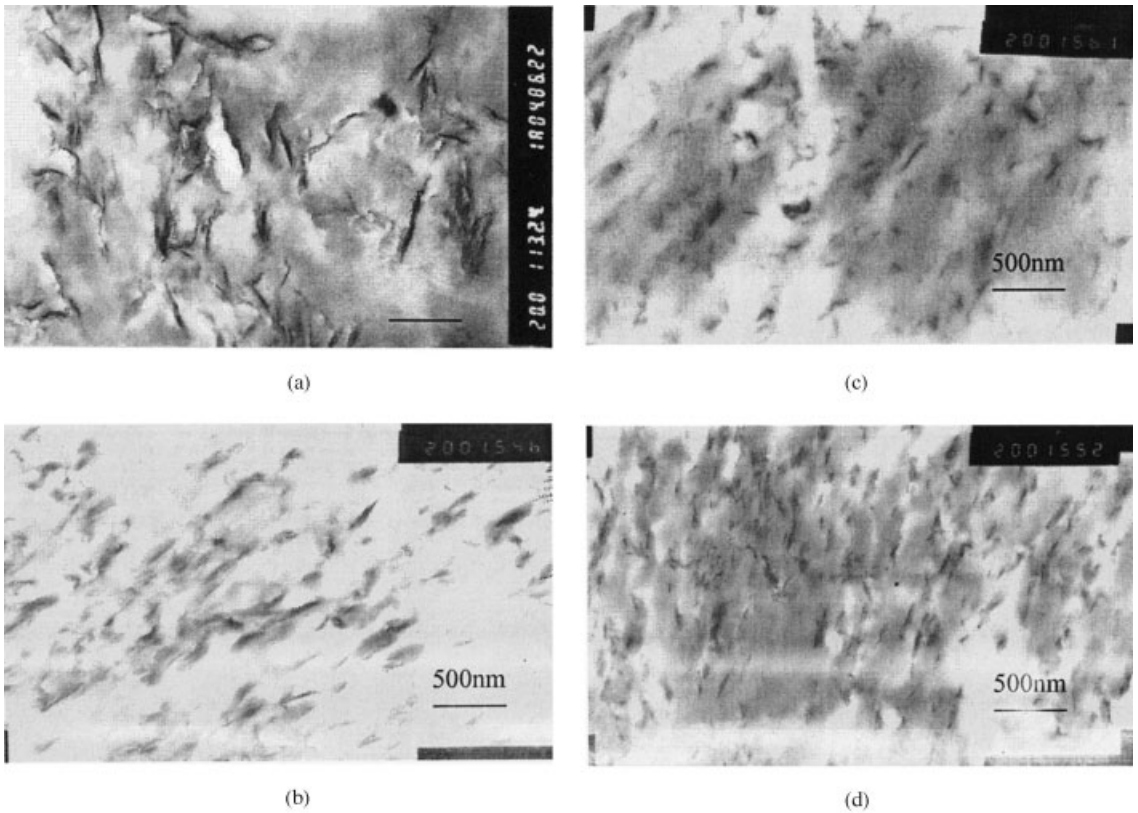

Figure 4 TEM images for hybrids of (a) BM, (b) BM-E, (c) BEM, and (d) B-EM at a magnification of 20,000×.

thickness reduces, as shown in Figure 4(b). It indicates that, although there is little difference between the expansion of the gallery heights in BM and BM-E hybrids, there are more polymer chains intercalated into the clay galleries in BM-E hybrid, and many tactoids are peeled to the smaller ones with the addition of epoxy as a compatilizer in the second melt process. This change in size of tactoids is more remarkable in BEM and B-EM hybrids, seen in Figures 4(c) and 4(d), indicating that the compatible effect by epoxy is more effective in preparation method of BEM and B-EM hybrids than in that of BM-E hybrid, and as a result, there are more clay tactoids dispersed in the matrix in smaller thickness. Therefore, although the XRD results show that all the hybrids have an intercalated structure, the dispersion of clay in the matrix, i.e., the amount and average size of tactoids, are various remarkably, which result in the different viscoelastic behavior in the lower frequencies.

The dynamic modulus of a polymer/compatilizer/clay nanocomposite can be described as follows:[13,21]

$$G'_{\text{nano}} = G'_{\text{matrix}} + G'_{\text{con}} + G'_{\text{inter}} + G'_{\text{com}} \quad (1)$$

the contribution of intercalated clay to G'_{nano} of the nanocomposites can be analyzed as follows: the confinement effect G'_{con} arises from the confinement of silicate layers with an interlayer distance smaller than or of the same order of the size of the chain coils, which may lead to the alternation of the relaxing dynamic of the intercalated polymers; and the interparticle interactions G'_{inter} comes from frictional interactions between the tactoids,[26] which result in the enhancement of low-frequency G'_{nano} in comparison with the polymer matrix G'_{matrix}. The term G'_{com} arises from the enhancement of the interfacial interaction between the polymer chain and clay tactoids due to the compatilizer.

As analyzed in TEM results, in contrast to the preparation of BM-E, to mix PBT, epoxy, and organoclay in one step can improve the compatibility between the matrix and the clay phase more effectively, resulting in the formation of much more smaller tactoids detached from the big ones. Therefore, the percolated clay network will evolve into the one with more perfect form and compact structure because of the enhancement of networks density, and as a result, the contribution of G'_{inter} in the BEM hybrid increases and the low-frequency G' enhances sharply due to the stronger physical jamming between the tactoids themselves than that in BM-E hybrids.

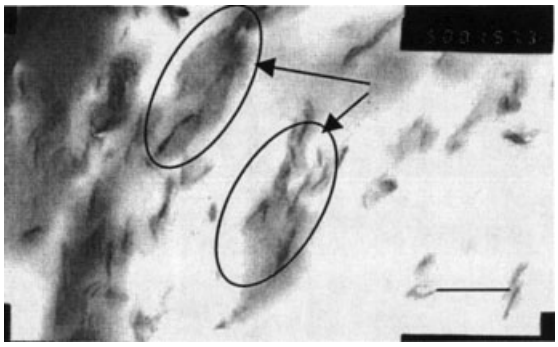

Figure 5 TEM images of B-EM hybrid at a magnification of 50,000×.

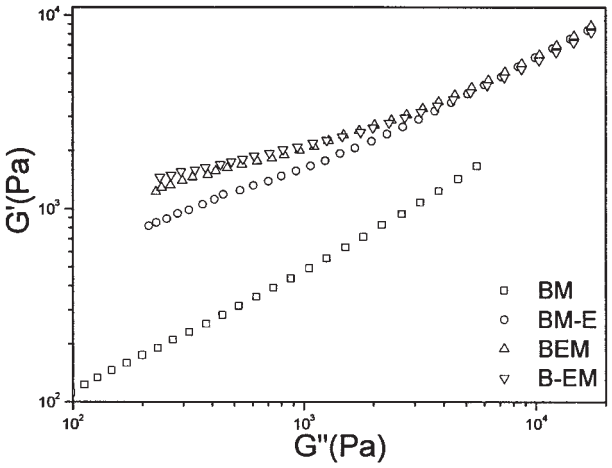

Figure 6 Plots of G' versus G'' for the hybrids.

As for B-EM hybrid, on the one hand, the first step of premixing epoxy and clay contributes to the formation of more amounts of tactoids than those in BEM and BM-E hybrids, leading to a more effective load transferability and enhancing the density of percolation network; On the other hand, as mentioned in the results from dynamic strain scan measurements, the enhancement of the hydrogen bonding between PBT chain and hydroxyl groups in tactoids surface can associate the tangled polymer chain network with that of percolated tactoids more tightly, resulting in an increase in G'_{com}.

Furthermore, many matrix chain bundles can surround several tactoids and link them up through hydrogen bonding and chain extension reaction,[25] which results in formation of flocculated structure of tactoids, as can be seen in Figure 5 (see the arrows). Figure 6 gives the curves of G' versus G''. As can be seen in Figure 6, BM hybrid presents a nice linear relationship between dynamic modules, which indicates that the physical adsorption between clay tactoids and PBT matrix nearly has no influence on the relaxation behavior of composite. However, the curves for the other three hybrids comprising epoxy present a deviation from linear relationship, especially in low-frequency zone. This trend elucidates some weak bond (hydrogen bonding) or chemical bond (chain extension reaction) does exist in between matrix and

tactoids or among tactoids themselves, which further confirms the formation of flocculated tactoids structure.

The existence of the flocculated structure leads to increasing in radius of the hydrodynamic volume of tactoids in some extent, raising the collision probability and friction intensity. Moreover, the relationship between tactoids inside the flocculated structure is much stronger than physical adsorption and friction. On the basis of the deviation level showed in Figure 6, it can be found that the flocculation degree in B-EM hybrids is highest of all the hybrids. Therefore, at the low frequencies, both the contribution of G'_{inter} and G'_{com} for B-EM hybrid are larger than those of BE-M and BEM hybrids. For these two factors, the B-EM hybrid exhibits a largest dynamic storage modulus and complex viscosity in the terminal zone, as shown in Figures 3 and 7.

In general, the two curves of storage and loss moduli do not intersect at the low frequencies, and for the most of polymer matrix, G'' is always higher than G'. However, the curves of polymer/clay nanocomposites exhibit an intersection due to the sharp enhancement of the G' value at the low frequencies, resulted from formation of the percolated tactoids network. (See the arrows in Fig. 3). In other words, at the crossover of the curves for storage modulus and loss modulus, phase angle δ is 45°, which means that the melt viscoelastic properties of the nanocomposites are suffering a transformation from the solid-like behavior to a liquid-like one at the point.

To a polymer/compatilizer/clay nanocomposite, the location of the point will be influenced by two factors: the compatibilization and plasticizing effect by compatilizer.[22] Since all these three hybrids have the identical epoxy content, the location of intersection can be regarded as an evaluation on the morphologies in nanocomposites. The frequencies located in 45° phase angle for all the hybrids are listed in Table II. Apparently, the value of $\omega_{\delta=45°}$(Hz) for B-E M hybrids is the largest one and around 1 Hz, which illuminates that the B-EM hybrid has the strongest percolated clay network due to the enhancement of network density and intensity. Therefore, the results from SAOS measurements are in consistent with those from TEM images.

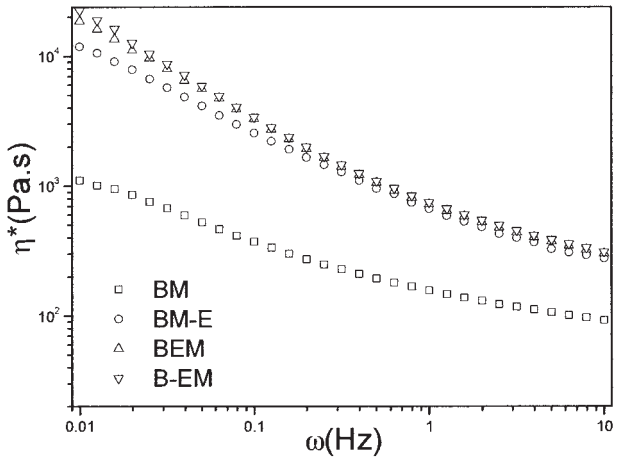

Figure 7 Comparison of dynamic complex viscosity of the hybrids.

TABLE II
The frequencies Located in 45° Phase Angle for the Hybrids

Samples	$\omega\delta$ = 45° (Hz)
BM	0.08
BM-E	0.57
BEM	0.85
B-EM	1.02

CONCLUSIONS

Nanocomposites, based on PBT/epoxy/organclay, were prepared through three different blending sequences in a Haake rheocord mixer : (1) to mix PBT, epoxy, and organoclay in one step; (2) first to mix epoxy and organoclay, then mix it with PBT; (3) to prepare PBT/organoclay hybrid first, and then mix it with epoxy to get the final nanocomposites. Although the XRD results show that all the hybrids have an intercalated structure, it is found that the mixing sequence influences the dispersion of clay in the matrix remarkably by the rheological approach, which are further proved through TEM images.

References

1. Kim, J. K.; Lee, H. Y. Polymer 1996, 37, 305.
2. Chisholm, B. J.; Fong, P. M.; Zimmer, J. G.; Hendrix, R. J Appl Polym Sci 1999, 74, 889.
3. Yang, J. H.; Shi, D.; Gao, Y.; Song, Y. X.; Yin, J. H. J Appl Polym Sci 2003, 88, 206.
4. Kojima, Y.; Usuki, A.; Kawasumi, M.; Okada, A.; Kurauchi T.; Kamigaito O. J Polym Sci Part A: Polym Chem 1993, 31, 983.
5. Wu, Z. G.; Zhou, C. X.; Qi, R. R.; Zhang, H. B. J Appl Polym Sci 2002, 83, 2403.
6. Wu, Z. G.; Zhou, C. X. Polym Test 2002, 21, 479.
7. Krishnamoorrti, R.; Vaia, R. A.; Giannelis, E. P. Chem Mater 1996, 8, 1728.
8. Vaia, R. A.; Janndt, K. D.; Kramer, E. J. Macromolecules 1995, 28, 8080.
9. Kawasumi, M.; Hasegawa, N.; Kato, M.; Usuki, A.; Okada, A. Macromolecules 1997, 30, 6333.
10. Usuki, A.; Kato, M.; Okada, A.; Kurauchi, T. J. J Appl Polym Sci 1997, 63, 137.
11. Galgali, G.; Ramesh, C.; Lele, A. Macromolecules 2001, 34, 852.
12. Li, J.; Zhou, C. X.; Wang, G. J Appl Polym Sci 2003, 89, 3609.
13. Li, J.; Zhou, C. X.; Wang, G.; Zhao, D. J Appl Polym Sci 2003, 89, 318.

14. Tyan, H. L.; Liu, Y. C.; Wei, K. H. Polymer 1999, 40, 4877.
15. Lan, T.; Kaviratna, P. D.; Pinnavaia, T. J. J Phys Chem Solids 1996, 57, 6.
16. Ma, J.; Zhang, S.; Qi, Z. N. J Appl Polym Sci 2001, 73, 1444.
17. Ke, Y. C.; Long, C. F.; Qi, Z. N. J Appl Polym Sci 1999, 71, 1139.
18. Li, X. C.; Kang, T.; Cho, W. J.; Lee, J. K.; Ha, C. S. Macromol Rapid Commu 2001, 21, 1306.
19. Chisholm, B. J.; Moore, R. B.; Barber, G.; Khouri, F.; Hempstead, A.; Larson, M.; Olson, E.; Kelley, J.; Balch, G.; Caraher, J. Macromolecules 2002, 35, 5508.
20. Li, X. C. Polym Eng Sci 2002, 42, 2156.
21. Wu, D. F.; Zhou, C. X.; Xie, F.; Mao, D. L.; Zhang, B. J Eur Polym 2005, 41, 2199.
22. Wu, D. F.; Zhou, C. X.; Zheng, H.; Mao, D. L.; Zhang, Polym Degrad Stab 2005, 87, 511.
23. Wu, D. F.; Zhou, C. X.; Xie, F.; Mao, D. L.; Zhang, B. Polym Polym Compos 2005, 13, 61.
24. Guo, B. H.; Chan, C. M. J App Polym Sci 1999, 71, 1827.
25. Wu, D. F.; Zhou, C. X.; Xie, F.; Mao, D. L.; Zhang, B. J Polym Sci Part B: Polym Phys, to appear.
26. Wei, Y.; Wu, Z. G.; Zhou, C. X. Chem J Chinese Universities 2003, 24, 715.